A bilayer scaffold of collagen and nanohydroxyapatite promotes osteochondral defect in rabbit knee joints

From Chang An District Hospital, Xi'an, China

Cite this article:
Bone Joint Res 2025;14(2):
155–165.

DOI: 10.1302/2046-3758.
142.BJR-2024-0171.R1

Correspondence should be sent to Shequn Zhang
doctorqsz@163.com

Y. Guo,[1,2,3] X. Peng,[1] B. Cao,[4] Q. Liu,[1] S. Li,[1,2] F. Chen,[1] D. Zhi,[1,2] S. Zhang,[1,2] Z. Chen[1]

[1]Northwest University Chang An Hospital, Faculty of Life Sciences and Medicine, Northwest University, Xi'an, China
[2]Chang An District Hospital, Xi'an, China
[3]Engineering Research Center of Oral and Maxillary System Disease, School of Stomatology, Xi'an Medical University, Xi'an, China
[4]Jiangsu DiYun Medical Technology Co., Ltd, Suzhou, China

Aims

A large number of surgical operations are available to treat osteochondral defects of the knee. However, the knee joint arthroplasty materials cannot completely mimic the articular cartilage and subchondral bone, which may bring some obvious side effects. Thus, this study proposed a biocompatible osteochondral repair material prepared from a double-layer scaffold of collagen and nanohydroxyapatite (CHA), consisting of collagen hydrogel as the upper layer of the scaffold, and the composite of CHA as the lower layer of the scaffold.

Methods

The CHA scaffold was prepared, and properties including morphology, internal structure, and mechanical strength of the CHA scaffold were measured by scanning electron microscopy (SEM) and a MTS electronic universal testing machine. Then, biocompatibility and repair capability of the CHA scaffold were further evaluated using a rabbit knee cartilage defect model.

Results

The CHA scaffold was well suited for the repair of articular cartilage and subchondral bone; the in vitro results showed that the CHA scaffold had good cytocompatibility. In vivo experiments demonstrated that the material had high biocompatibility and effectively induced cartilage and subchondral bone regeneration.

Conclusion

The CHA scaffold has a high potential for commercialization and could be used as an effective knee repair material in clinical applications.

Aricle focus

- The preparation method of a double-layer scaffold of collagen and nanohydroxyapatite (CHA), consisting of collagen hydrogel as the upper layer of the scaffold and the composite of collagen-nanohydroxyapatite as lower layer of the scaffold.
- The verification of the repair function of CHA scaffold.

Key messages

- The CHA scaffold was shown to be well suited for the repair of articular cartilage and sub chondral bone.
- The CHA scaffold has good cytocompatibility and biocompatibility.
- In vivo experiments demonstrated that the CHA scaffold effectively induces cartilage and subchondral bone regeneration.

Strengths and Limitations

- The CHA scaffold has a strong repair effect in cartilage and subchondral bone defects.
- Larger animal studies are needed to validate the CHA scaffold before it can be used in clinical applications of knee repair.

Bone & Joint Research

Introduction

Trauma, osteochondritis dissecans (OCD), subchondral bone hypoplasia fractures, or damage to the subchondral bone plate from previous surgeries can cause osteochondral injuries in the knee. Such localized abnormalities in the subchondral bone and articular cartilage can lead to substantial joint pain and morbidity over time. In some cases, up to 60% of knees are found to have such defects at the time of arthroscopy.[1-3] Several intra-articularly administered drugs, such as corticosteroids,[4] hyaluronic acid,[5] glucosamine,[6] and antibiotics[7] have been used clinically. However, long-term injection of corticosteroids in articular cavities can lead to the imbalance of cartilage metabolism and osteoporosis. Intra-articular injections of hyaluronic acid lubricate joints and relieve pain and other symptoms, but cannot repair cartilage damage. Thus, the long-term clinical outcomes remain controversial.[8] When these lesions are symptomatic and fail nonoperative management, surgical strategies are available. Hydroxyapatite (HA)-coated titanium femoral components,[9-12] acetabular components,[13,14] and cemented hemiarthroplasty[15] have been used in hybrid total hip arthroplasty. The HA has a natural affinity for bone cells and tissues, which is conducive to the rapid combination of bone tissue with the scaffold to fix the upper layer cartilage tissue. However, surgical treatment is not effective in healing articular cartilage defects, and the quality of regenerated cartilage is poor.[16] Extracorporeal shockwave therapy (ESWT) was reported to promote the effect of TGF-β/BMPs, thereby modulating the production of extracellular matrix (ECM) proteins and transcription factors involved in the regeneration of articular cartilage and subchondral bone, in an OCD rat model.[17]

Osteochondral allograft transplantation presents a promising treatment option.[18] Autologous matrix-induced chondrogenesis (AMIC) has been considered as an encouraging treatment option for large cartilage lesions of the hip.[19] However, the allografts have a limited source. The scaffolds provide structural support and space for regeneration of surrounding tissues and cell growth.[20] The scaffolds are often prepared from natural and synthetic materials. Natural materials such as ECM, with good biocompatibility and degradability, can promote cell adhesion, migration, differentiation, and ECM deposition. Synthetic materials are also widely used because of their controllable mechanical and degradation properties. However, their hydrolysis reaction during in vivo degradation may cause local pH reduction and inflammatory reactions.[21] Moreover, due to the normal cartilage and bone having completely different mechanical stiffness and material structural properties,[22] repairing osteochondral defects is difficult and complicated. Common materials used to prepare monophasic scaffolds include collagen,[23] HA ($Ca_{10}(PO4)_6(OH)_2$, HA), and some synthetic polymers.[24,25] The collagen has advantages in chondrocytes, and thus monophasic scaffolds made from collagen have often been studied in cartilage defect repair. Onodera et al[26] reported that ultra-purified alginate (UPAL) gel was implanted and facilitated cartilage repair. Helwa-Shalom et al[27] found that 0.5 μg/μl recombinant human amelogenin protein (rHAM) induced in vivo healing of injured articular cartilage and subchondral bone in a rat model. The double-layer scaffold has attracted much attention due to its advantages. However, this double-layer scaffold still had many defects that prevented it from being used in in vivo experiments. For example, it has been reported that the difficulty of simultaneous growth of cartilage and bone in the same culture media made it impossible to achieve the co-culture of more than one type of cell on the same composite scaffolds.[28] All of these problems have prevented the study of the bipolar collagen/HA scaffold until now; we developed the novel double-layer collagen nanohydroxyapatite scaffold (CHA) for in situ osteochondral repair.

In this study, we designed a novel scaffold with an upper pure collagen layer corresponding to the cartilage region, and a lower CHA composite layer that mimics the subchondral bone. The key point is that in the surgical method, we drilled a hole in the articular surface to reach the bone marrow cavity, and then the bone marrow mesenchymal stem cells (BMSCs) could be released, and the growth factors in the bone marrow would also be absorbed into the collagen sponge, to achieve the perfect integration of seed cells and growth factors with the scaffold and the in situ repair of the scaffold at the tissue damage site.

Methods

Preparation for CHA scaffold

The method of extraction of rat tail collagen was performed as follows.[29] The rat tails (n = 50) were collected and soaked in 75% alcohol after washing. The tail tendon was obtained, washed in phosphate-buffered saline (PBS), and then weighed and cut into 2 to 3 mm fragments, and soaked in 0.1% acetic acid solution at a concentration of 50 ml/g. Then it was placed at 4°C for one week, during which it was shaken four to six times a day. Next, the supernatant was obtained by centrifugation (4°C, 4,000 rpm, 30 mins). Then, 0.1% acetic acid solution was added again into the precipitation and placed at 4°C for two to three days. The supernatant was obtained by centrifugation again (4°C, 4,000 rpm, 30 mins), and then we obtained the crude-extracted collagen. Then, 2 mol/l NaCl solution equal to the supernatant was added at a ratio of 1:1 for salting out. The precipitation was obtained by 4°C centrifuge again at 4,000 rpm for 30 minutes, and cleaned with sterile ddH_2O to remove the residual salt ions. Then it was re-suspended and precipitated with 0.1% acetic acid solution. Finally, rat tail collagen was obtained through overnight freezing at -80°C, and freeze-dried in a vacuum freeze dryer.

The synthetic process of the CHA scaffold is illustrated in Figure 1. The collagen obtained was weighed at 0.4 g and dissolved in 20 ml 0.1% acetic acid solution for 20 mg/ml collagen solution. The pH of the collagen solution was adjusted to neutral with 1 M NaOH solution and stirred with a magnetic stirrer at 4°C until it was completely dissolved. Then, 0.5 g nano-HA was added into the collagen solution, thoroughly mixed with a vortex oscillator, and added into a 96-well plate to 100 μl per well, frozen at -20°C for two hours, and then frozen at -80°C overnight. Next, the 96-well plate was taken out, and 100 μl of 20 mg/ml collagen solution was added to the frozen composite of CHA when it began to melt. Finally, it was placed at -80°C and dried in a vacuum freeze dryer.

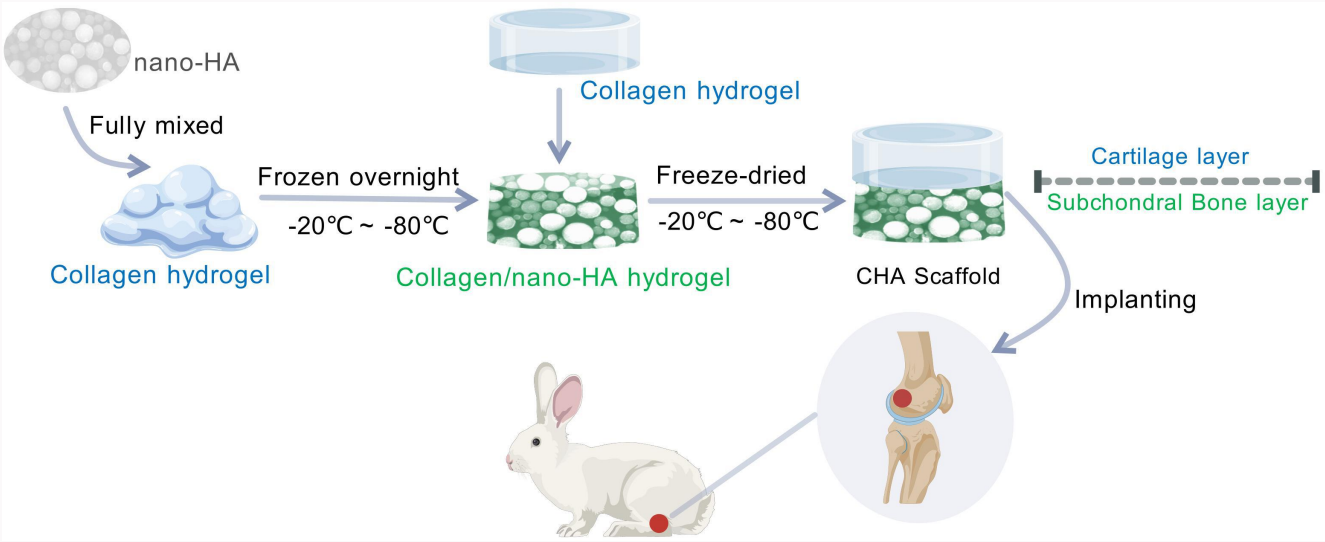

Fig. 1
Preparation diagram of collagen nanohydroxyapatite (CHA) scaffold. The collagen obtained was mixed with hydroxyapatite (HA) and gradient frozen overnight, then collagen solution was added to the frozen material, which continued de-gradient freezing and was dried in a vacuum freeze dryer.

SEM of CHA scaffold

The collagen scaffold, HA and CHA scaffolds were freeze-dried, cut, and sprayed with gold for 150 seconds using an ion sputter (Cressington, China) with a parameter of 30 mA, 150 V. Then, the microstructure of the CHA scaffold was observed by scanning electron microscopy (SEM; JSM-7001F; Nippon Electronics, Japan).

Mechanical property of CHA scaffold

The height and diameter of material samples were measured by a vernier caliper before being placed on the fixture of the MTS electronic universal testing machine (MTS-858 Mini Bionix II; MTS Systems, USA). Then, pre-load was set at -0.3 N and the samples were compressed at a loading rate of 0.033 mm/s, until the sample was damaged. Five independent samples were used to evaluate the mechanical properties. The elastic modulus was calculated as follows: E = stress/strain (stress =ΔF/S, strain =ΔL/H).

Water contact angle of CHA scaffold

To evaluate the surface wettability and hydrophilicity of scaffolds, the collagen scaffold and HA and CHA scaffolds were prepared and tested using a water contact angle tester (LSA60; LAUDA Scientific, Germany). Briefly, the nano-HA, collagen solution, and CHA solution were spread on the slide and air-dried overnight in a fume hood. Then, the samples were tested and three points were made for every sample.

FITR of CHA scaffold

Since fourier-transform infrared spectroscopy (FTIR) is often used to investigate the different functional groups of the molecules, we tested the groups of nano-HA, collagen and CHA scaffolds by FTIR to detect whether CHA scaffold was successfully prepared. In brief, the nano-HA, collagen solution, and CHA solution were placed on the surface of slides and air-dried in the fume hood overnight. Then, the samples were tested and analyzed by FTIR (IRTracer-100; Shimadzu, Japan).

Cell proliferation

Rabbit BMSCs and chondrocytes were isolated according to our previous method.[30,31] BMSCs (2×10^4 cells/ml) and chondrocytes (2×10^4 cells/ml) were seeded into 96-well plates (150 μl per well) and cultured for six hours. Next, sterilized CHA or collagen scaffolds were added in the culture plate, and then were co-cultured with cells for one, two, and three days. For each timepoint, 10% Cell Counting Kit-8 (CCK-8) was added to react for two hours, and then 100 μl was placed in the 96-well plate and measured by an enzyme-labelled instrument (ELx800; BioTek, USA) at a wavelength of 450 nm, with six duplicatesset for every group. Meanwhile, BMSCs and chondrocytes were seeded into six-well plates and cultured with sterilized collagen/HA or collagen scaffolds, respectively. Then, the rabbit BMSCs and chondrocyte cells were all stained with neutral red to observe cell proliferation after being cultured for one or three days.

Cell migration

We further tested the effect of CHA on cell migration. Briefly, 5×10^5 BMSCs and chondrocytes were seeded into each well of the six-well plate and cultured for six hours. After the cells had almost covered the bottom of the wells, starvation incubation with 0.5% fetal bovine serum (FBS) medium was continued for 12 hours. A 10 μl sterile tip was then used to draw a straight line across the bottom of the cell-lined six-well plate. The wells were washed three times with PBS, and then both BMSCs and chondrocyte cells were cultured for an additional 12 hours in Dulbecco's Modified Eagle Medium (DMEM) with the CHA or collagen scaffolds, respectively, and cells cultured in DMEM acted as a control. Cells were then stained with crystal violet. Images were recorded at 0 hours and 12 hours for analysis. The migration area between migrating edge and wound edge was measured using ImageJ software (National Institutes of Health, USA) and ten duplicates were set for every group.

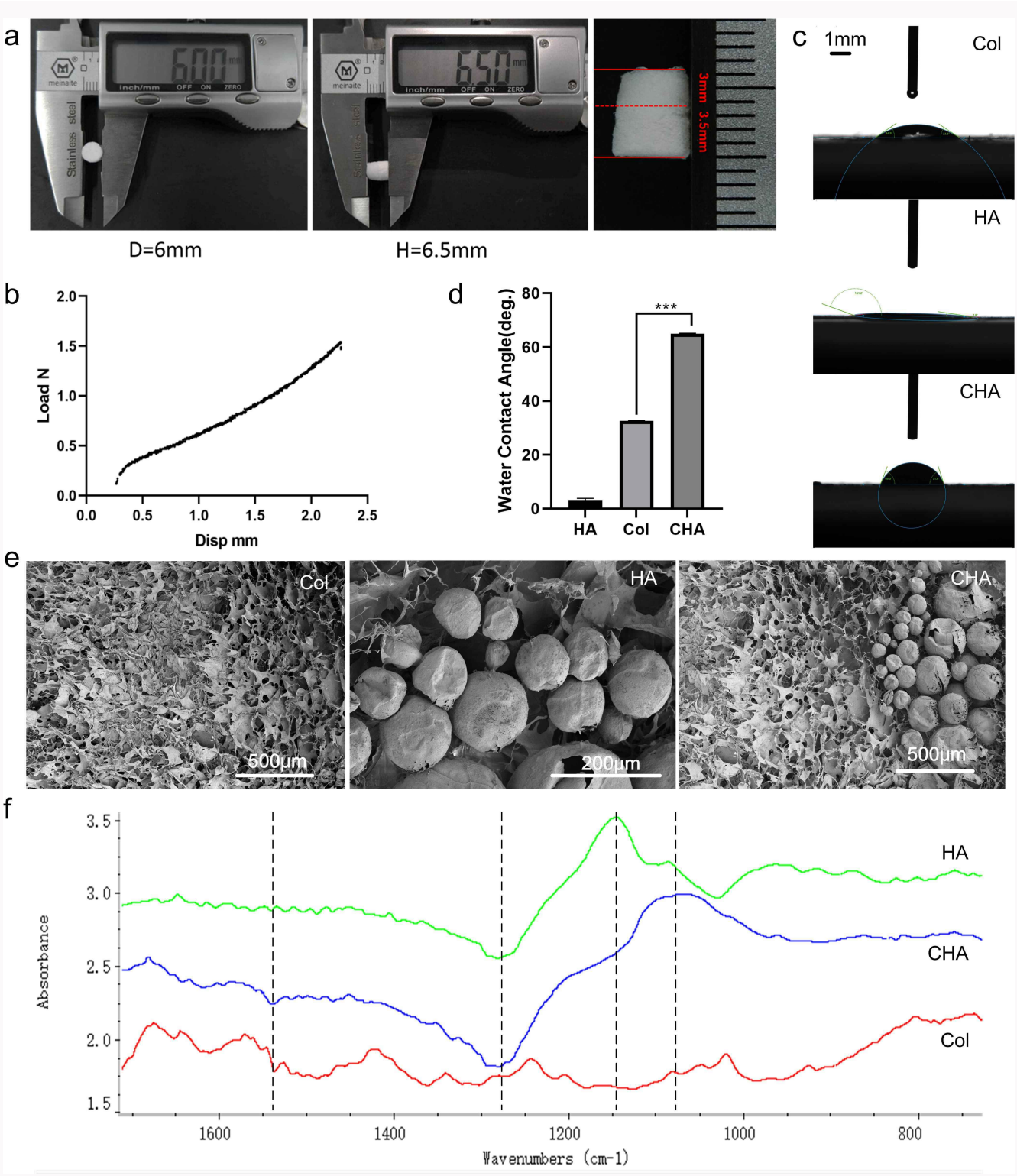

Fig. 2

Characterization of collagen nano-hydroxyapatite (CHA) scaffolds. a) Morphological observation of double-layer scaffold of CHA. b) Mechanical property of CHA scaffolds. c) and d) Water contact angle of collagen, hydroxyapatite (HA), and CHA scaffold. e) Scanning electron microscopy (SEM) images of CHA scaffolds. f) Fourier-transform infrared spectroscopy (FITR) of collagen, HA, and CHA scaffold.

Articular joint drilling surgery

Ten New Zealand white rabbits (three months old, male:female = 1:1) were randomly divided into two groups: control group (n = 3) and CHA group (n = 7). The specific procedures were as follows: the rabbits were weighed and anaesthetized with 25% ethyl carbamate auricular vein (600 to 800 mg/kg). After removing fur from the right hind leg of the rabbit, the osteochondral defect model of the knee joint was created according to our previous study.[32] Then, CHA scaffolds were carefully placed into the osteochondral defects and sutured closely, while the control group received no treatment. The authors adhered to the ARRIVE guidelines for animal studies, and have included an ARRIVE checklist in the Supplementary Material.

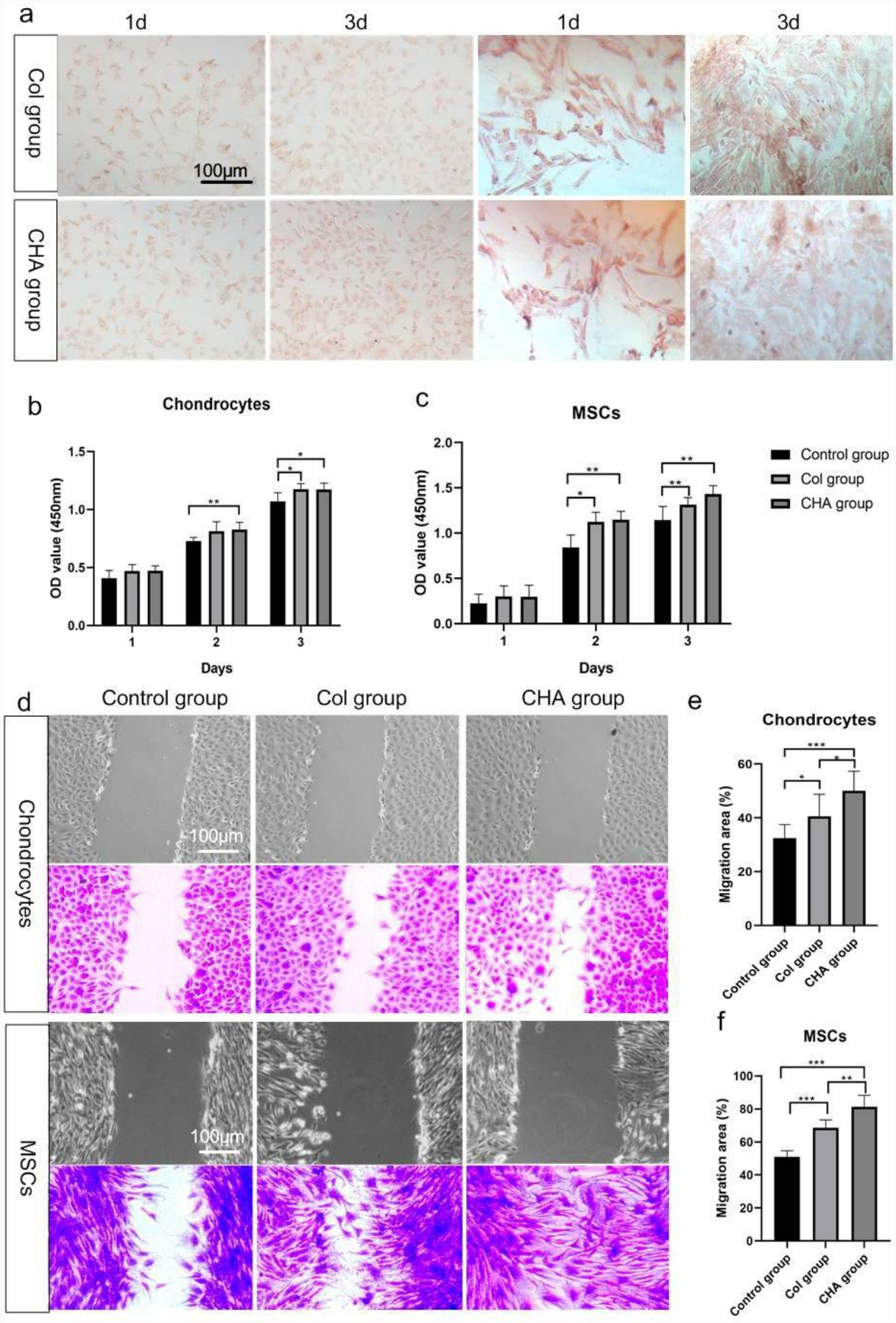

Fig. 3

Biocompatibility of collagen (Col) nano-hydroxyapatite (CHA) scaffolds. a) Neutral red staining of bone marrow mesenchymal stem cells (BMSCs) and chondrocytes in the medium containing collagen scaffolds or CHA scaffold. b) and c) Cell Counting Kit-8 (CCK-8) assay was used to test the effect of collagen scaffold and CHA scaffold on cell proliferation, containing chondrocytes and BMSCs. d) Observation of cell migration in the collagen scaffold and CHA scaffold medium. e) and f) Quantification of migration area rate on BMSCs and chondrocytes cultured in the medium containing collagen scaffold or CHA scaffold. OD, optical density.

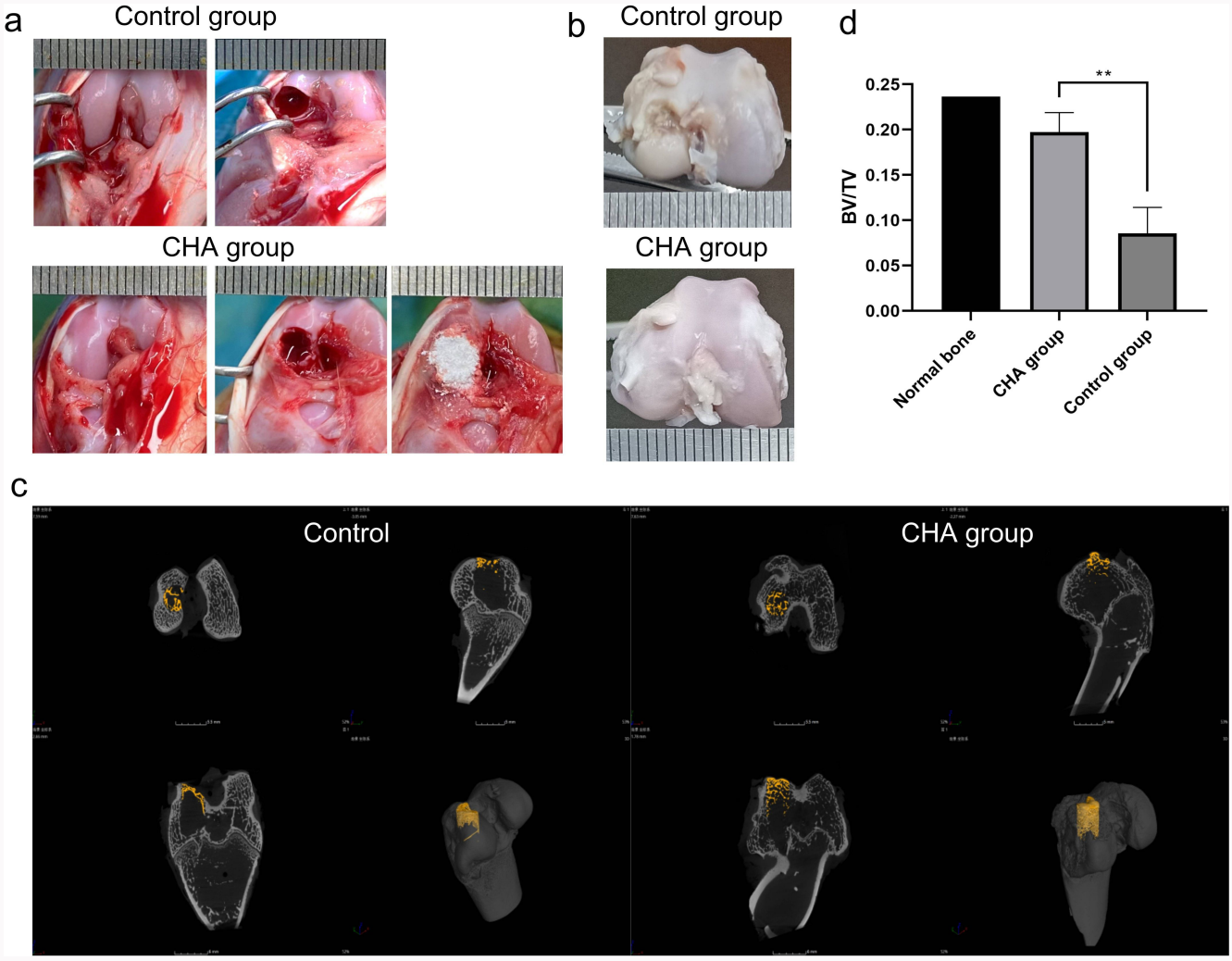

Fig. 4
Evaluation of collagen nano-hydroxyapatite (CHA) scaffold on chondral injury. a) Model of knee joint cartilage defect. b) Gross observation of the repaired cartilage tissues two months postoperatively. c) Micro-CT of new regenerated bone. d) Quantification of bone volume/total volume (BV/TV).

CT observation

Two months after surgery, all rabbits were killed, and the bone tissues were obtained and fixed in 4% paraformaldehyde. Then, the morphological and quantitative examination of bone tissue samples was completed using micro-CT (SkyScan 1272; Bruker, Germany), and the bone volume fraction (BVF) was calculated to evaluate bone defect repair.

Histological and immunofluorescence observation

The bone tissue samples were taken out from 4% paraformaldehyde, washed with PBS, and decalcified in ethylenediaminetetraacetic acid (EDTA) decalcified solution. Samples were then graded and dehydrated in ethanol, embedded in paraffin, and sectioned. To evaluate new cartilage and bone formation, the sections were analyzed using haematoxylin and eosin (H&E), Masson's trichrome staining (MTS), Toluidine blue (TB), and safranin O (S-O) staining. To further evaluate the bone tissue repair, immunofluorescence staining was performed. Briefly, the slices were incubated with primary antibodies (anti-Col I for BMSCs, anti-Col II for chondrocytes), rinsed with PBS, and then incubated with secondary antibody (Alexa Fluor 488; Thermo Fisher Scientific, USA) and 4',6-diamidino-2-phenylindole (DAPI). The images of the stained slices were taken by a confocal laser scanning microscope (FV1000; Olympus, Japan).

Statistical analysis

All data in experiments are presented as mean and SD. The migration area was calculated by ImageJ, and statistical analysis was performed using SPSS Statistics v22 (IBM, USA) software. The statistical differences were analyzed by one-way analysis of variance (ANOVA), and $p < 0.05$ was considered to be statistically significant.

Results

Preparation and characterization of CHA scaffold

As shown in Figure 2a, the CHA scaffolds with a height of 6.5 mm and a diameter of 6 mm have an obvious stratification, consisting of a 3 mm collagen layer and a 3.5 mm CHA layer. Results of mechanical properties showed that incorporation of nano-HA into collagen hydrogels increased the elastic moduli of the CHA scaffolds, with elastic moduli of CHA scaffold reaching up to a mean 0.196 MPA (SD 0.005) (Figure 2b). After nano-HA, the hydrophilicity of the collagen surface was altered (Figure 2c), and the results of mean water contact angles showed that all the material surfaces (HA: 3.24° (SD

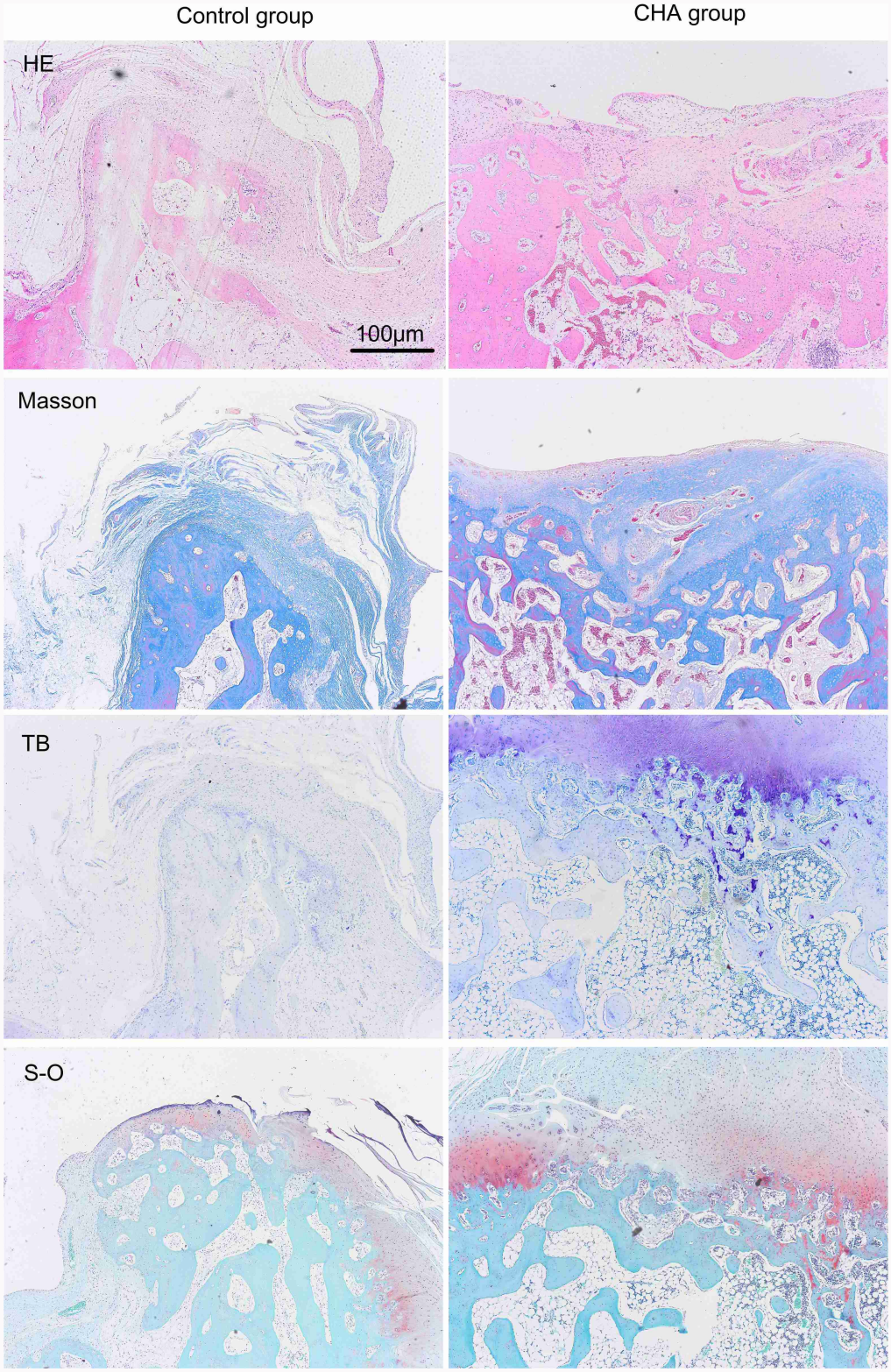

Fig. 5
Histological staining of bone tissues. CHA, collagen-nanohydroxyapatite scaffold; HE, haemotoxylin and eosin; Masson, Masson's trichrome staining; S-O, safranin O; TB, Toluidine blue.

0.60°); collagen: 32.57° (SD 0.12°); collagen/HA: 65.00° (SD 0.17°)) were hydrophilic, which is beneficial for cell adhesion (Figure 2d). As shown in SEM images, the upper layer of CHA scaffolds had a loose and porous structure, while the lower layer of CHA scaffolds showed nano-HA in porous collagen hydrogels and physically adhered to collagen hydrogel in the CHA scaffold (Figure 2e). The chemical structure change of the collagen scaffolds after adding HA was further investigated by FTIR, and results indicated that both collagen/nano-HA and collagen had a peak at 1,530 cm^{-1} corresponding to the in-plane bending vibration (δ) of N–H (amide II), and both collagen/nano-HA and HA had a peak at 1,275 cm^{-1}, while

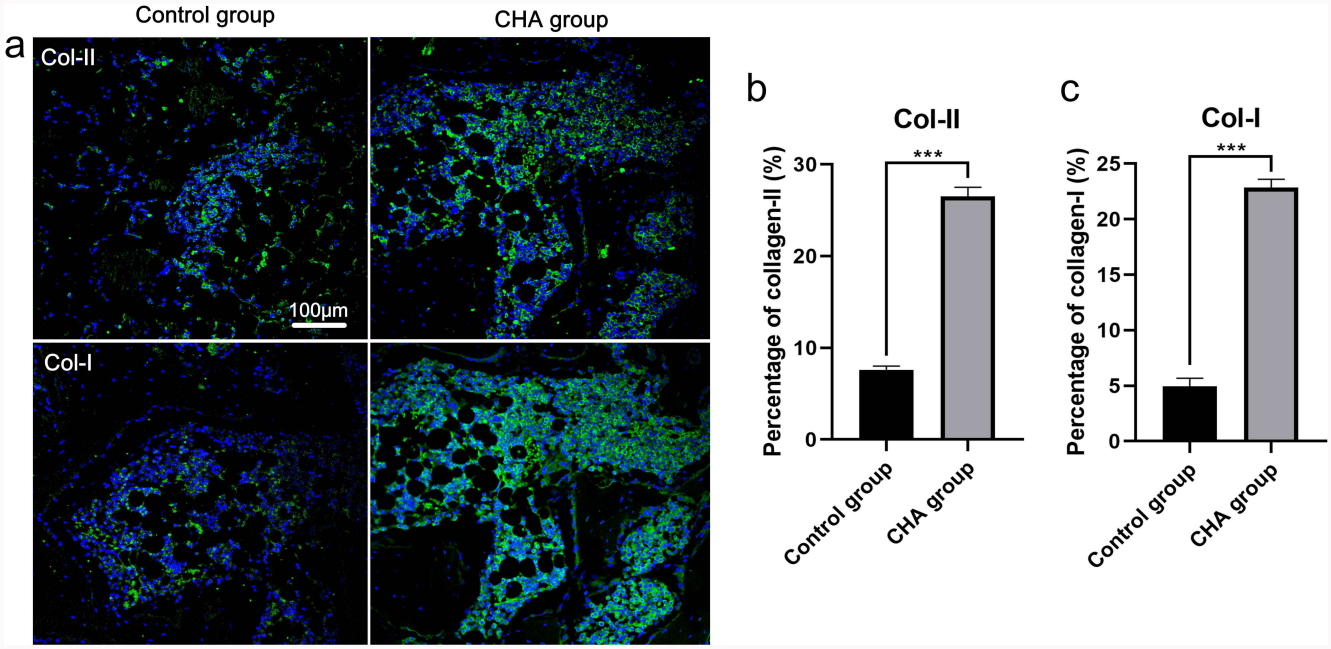

Fig. 6
Histological staining of bone tissues. a) Immunofluorescence staining of new bone tissue with collagen II and collagen I. Quantitative analysis of b) collagen II and c) collagen I positive area. CHA, collagen-nanohydroxyapatite scaffold.

collagen/nano-HA increased to a new peak at 1,069 cm^{-1} corresponding to ν C–N (Figure 2f). These results demonstrate that the collagen/HA have formed new bonds to improve mechanical properties.

Biocompatibility of CHA scaffolds on bone defects

Any biomaterials applied to osteochondral defects of the knee repair must be biocompatible. The effect of CHA scaffold and collagen scaffold on cell proliferation was evaluated by neutral red staining and CCK-8 assay. The images of neutral red staining showed that BMSCs and chondrocytes could continue to grow and proliferate on CHA scaffold and collagen scaffold (Figure 3a). According to the results of CCK-8 assay on BMSCs and chondrocytes (Figures 3b and 3c), the OD_{450} value between the CHA group and control group showed a significant difference, indicating that CHA promoted cell proliferation. In addition, the cell wound scratch assay was performed to test whether the CHA scaffold promotes BMSC and chondrocyte migration (Figures 3d to 3f). As shown in Figure 3d, BMSCs and chondrocytes migrated to the scratched region over time, and those co-cultured with CHA scaffold migrated faster than those cultured with collagen scaffold non-treatment after 12 hours. The quantification of migration area rate indicated that both CHA and collagen promoted cell migration, and that the CHA group had a greater promoting effect than the collagen group (Figures 3e and 3f).

Effect of CHA scaffolds on bone defects

As shown in Figure 4a, two months after surgery, it was observed that regenerated tissues in the CHA group were well integrated with the surrounding cartilage tissues, showing a white and smooth appearance, very similar to normal cartilage. In contrast, the control group still had significant defects, with little fibrous tissue at the base of the defective holes (Figure 4b). The results of micro-CT also showed that the osteochondral defects in the CHA group were replaced by more bone and cartilage-like tissue compared to the control group (Figure 4c). Additionally, the BVF values in the CHA group were higher than in the control group, which confirmed that CHA scaffold could promote articular osteochondral defect repair (Figure 4d).

Histological evaluation of collagen/nano-hydroxyapatite scaffold on bone defects

We observed from H&E staining images that there was more newly formed cartilage in the CHA group than in the control group. In vivo results were consistent with previous studies that type I collagen scaffolds supported chondrogenesis in vitro.[33,34] In addition, MTS, TB, and S-O staining further suggested that the CHA group formed a larger amount of cartilage collagen and polysaccharides than the control group, significantly promoting cartilage matrix formation in vivo (Figure 5). The in vivo results were also consistent with previous studies that individual type I collagen[35] or HA[36] substrates improved ability of osteoblast differentiation, and a combination of collagen-I and HA could accelerate osteogenesis.[37] The reason for this may be that the Col/HA composite is similar to bone tissue in composition and microstructure, providing an appropriate microenvironment for osteogenesis.[38]

Collagen deposition of new regenerated bone

Collagen II is one of the key proteins in the ECM of articular cartilage, while collagen I plays a key role in formation and maintenance of bone structure. To further evaluate the regenerated cartilage tissue, we also performed immunofluorescence staining of new bone tissue with collagen II and collagen I antibodies (Figure 6a). The quantitative analysis of the immunofluorescence images indicated that collagen II and collagen I deposits were significantly higher in the CHA group

than in the control group (Figures 6b and 6c). The capacity of repairing both articular and hypertrophic cartilage suggested that our CHA scaffolds possess potential for remodelling and repair of osteochondral defects.

Discussion

The composite scaffold scheme is not uncommon in the application of bone and cartilage medical tissue engineering. In order to overcome the limitations of conventional scaffolds such as poor biocompatibility, suboptimal mechanical properties, uncontrollable rate of biodegradation, and mismatch between a single structure and the layered structure of articular cartilage, hyaluronic acid was added to collagen to form a cylindrical structure in a previous study. This composite scaffold has good cell compatibility and stronger mechanical properties than pure collagen. However, the mechanical properties required for cartilage and subchondral bone repair are still not perfect.[39]

HA, the main component of bone powder, although its degradation rate is low,[40-42] has good mechanical properties, excellent biocompatibility with hard tissue,[43] and high bone conductivity and biological activity.[44] It is neither antigenic nor cytotoxic.[42] However, the single use of nano-hydroxyapatite (HA) as bone filling material is ineffective for bone repair and cannot achieve the desired repair effect because its powder is easily dispersed under the free flow of body fluids. Therefore, many researchers add polyester materials such as poly(lactic-co-glycolic acid) (PLGA) and polylactic acid (PLA) into HA powder to demonstrate that HA can form a unique shape and be fixed to the bone defect.[45] It is worth noting that polyester materials used more in the past can easily use 3D printing technology to achieve defect filling. However, polyester materials have limited ability to capture cells at bone repair sites due to their large hydrophobic properties and opposite hydrophilic environment in vivo, which also reduces the effect of bone repair.[46] In contrast, the addition of collagen to HA not only meets the characteristics of biocompatibility, biodegradability, and bone induction, but also prevents the dispersion of HA in the implant, thus forming a biomaterial that easily repairs bone defects.[28,47,48]

During the process of repairing osteochondral defects in knee joints, it is necessary to induce the formation of osteocytes to reach the state of bone repair, and to induce the formation of chondrocytes to reach the state of cartilage repair. The method of preventing the over-repair of either bone or cartilage, and thus balancing the degree of bone and cartilage repair, has become a challenge for researchers. In this study, the characteristics of collagen were fully utilized. Collagen and HA were mixed to condense HA in the lower scaffold, maintain good mechanical properties, and recruit and induce osteocytes in bone repair. At the same time, a separate rat tail collagen that was used as the upper layer provides a collagen fibre platform for the migration of chondrocytes and the reconstruction of the cartilage layer.[28] Zhou et al[28] performed in vitro studies comparing monophasic collagen scaffold and biphasic collagen/HA scaffolds, and the results showed that bipolar collagen/HA scaffold has more advantages in osteogenesis, while monophasic collagen scaffolds performed better in chondrogenesis. The experimental results also showed that the composite scaffold not only possesses positive mechanical properties for bone tissue repair, but also exhibited strong osteoinductive ability and inhibited cartilage calcification caused by excessive bone growth in the cartilage layer.

In conclusion, in our study we developed a novel CHA scaffold with a unique structure and properties that can effectively match and repair osteochondral defects in the knee joint. Additionally, the CHA scaffold could promote BMSC and chondrocyte proliferation and migration, suggesting good biocompatibility. Animal experiments indicated that our CHA scaffold induced cartilage and subchondral bone tissue recovery effectively. Because of the unique performance and high repair capability of CHA scaffolds, they have high clinical potential in joint defect repair.

Supplementary material

An ARRIVE checklist is included in the Supplementary Material to show that the ARRIVE guidelines were adhered to in this study.

References

1. **Chahla J**, **Stone J**, **Mandelbaum BR**. How to manage cartilage injuries? *Arthroscopy*. 2019;35(10):2771–2773.
2. **Frank RM**, **Cotter EJ**, **Hannon CP**, **Harrast JJ**, **Cole BJ**. Cartilage restoration surgery: incidence rates, complications, and trends as reported by the American Board of Orthopaedic Surgery Part II Candidates. *Arthroscopy*. 2019;35(1):171–178.
3. **Cavinatto L**, **Hinckel BB**, **Tomlinson RE**, **Gupta S**, **Farr J**, **Bartolozzi AR**. The role of bone marrow aspirate concentrate for the treatment of focal chondral lesions of the knee: a systematic review and critical analysis of animal and clinical studies. *Arthroscopy*. 2019;35(6):1860–1877.
4. **Li S**, **Zhang W**, **Lin Y**. Application of intra-articular corticosteroid injection in juvenile idiopathic arthritis. *Front Pediatr*. 2022;10:822009.
5. **Lin X**, **Zhi F**, **Lan Q**, **Deng W**, **Hou X**, **Wan Q**. Comparing the efficacy of different intra-articular injections for knee osteoarthritis: a network analysis. *Medicine (Baltimore)*. 2022;101(31):e29655.
6. **Feng X**, **Beiping L**. Therapeutic efficacy of ozone injection into the knee for the osteoarthritis patient along with oral celecoxib and glucosamine. *J Clin Diagn Res*. 2017;11(9):UC01–UC03.
7. **Ferguson J**, **Bourget-Murray J**, **Stubbs D**, **McNally M**, **Hotchen AJ**. A comparison of clinical and radiological outcomes between two different biodegradable local antibiotic carriers used in the single-stage surgical management of long bone osteomyelitis. *Bone Joint Res*. 2023;12(7):412–422.
8. **McAlindon TE**, **LaValley MP**, **Harvey WF**, **et al**. Effect of Intra-articular triamcinolone vs saline on knee cartilage volume and pain in patients with knee osteoarthritis: a randomized clinical trial. *JAMA*. 2017;317(19):1967–1975.
9. **Turgeon TR**, **Righolt CH**, **Burnell CD**, **Gascoyne TC**, **Hedden DR**, **Bohm ER**. Comparison of two hydroxyapatite-coated femoral components: a randomized clinical trial using radiostereometric analysis. *Bone Joint J*. 2023;105-B(10):1045–1051.
10. **Yee AHF**, **Chan VWK**, **Fu H**, **Chan P-K**, **Chiu KY**. Long-term follow-up of an uncemented proximally hydroxyapatite-coated femoral stem in total hip arthroplasty. *Bone Joint J*. 2024;106-B(3 Supple A):110–114.
11. **Upadhyay PK**, **Shah N**, **Kumar V**, **Mirza SB**. Hydroxyapatite ceramic-coated femoral components in younger patients followed up for 27 to 32 years. *Bone Jt Open*. 2024;5(4):286–293.
12. **Ohyama Y**, **Minoda Y**, **Masuda S**, **Sugama R**, **Ohta Y**, **Nakamura H**. Contact states with femoral cortical bone and periprosthetic bone mineral density changes differ between traditional and newly introduced fully hydroxyapatite-coated stems. *Bone Joint J*. 2024;106-B(6):548–554.
13. **Hamilton DF**, **Gaston P**, **Macpherson GJ**, **Simpson P**, **Clement ND**. Nexus Evaluation Primary Trident II UNcemented shEll (NEPTUNE). *Bone Jt Open*. 2023;4(10):782–790.

14. **van der Lelij TJN**, **Marang-van de Mheen PJ**, **Kaptein BL**, **et al**. Migration and clinical outcomes of a novel cementless hydroxyapatite-coated titanium acetabular shell: two-year follow-up of a randomized controlled trial using radiostereometric analysis. *Bone Joint J*. 2024;106-B(2):136–143.
15. **Parker MJ**, **Chatterjee R**, **Onsa M**, **Cawley S**, **Gurusamy K**. Cemented versus uncemented hemiarthroplasty for displaced intracapsular fractures of the hip. *Bone Joint J*. 2023;105-B(11):1196–1200.
16. **Ozmeriç A**, **Alemdaroğlu KB**, **Aydoğan NH**. Treatment for cartilage injuries of the knee with a new treatment algorithm. *World J Orthop*. 2014;5(5):677–684.
17. **Cheng J-H**, **Jhan S-W**, **Chen P-C**, **et al**. Enhancement of hyaline cartilage and subchondral bone regeneration in a rat osteochondral defect model through focused extracorporeal shockwave therapy. *Bone Joint Res*. 2024;13(7):342–352.
18. **Poursalehian M**, **Ghaderpanah R**, **Bagheri N**, **Mortazavi SMJ**. Osteochondral allografts for the treatment of shoulder instability. *Bone Jt Open*. 2024;5(7):570–580.
19. **Briem T**, **Stephan A**, **Stadelmann VA**, **et al**. Mid-term results of autologous matrix-induced chondrogenesis for large chondral defects in hips with femoroacetabular impingement syndrome. *Bone Joint J*. 2024;106-B(5 Supple B):32–39.
20. **Capito RM**, **Spector M**. Scaffold-based articular cartilage repair. *IEEE Eng Med Biol Mag*. 2003;22(5):42–50.
21. **Getgood A**, **Brooks R**, **Fortier L**, **Rushton N**. Articular cartilage tissue engineering: today's research, tomorrow's practice? *J Bone Joint Surg Br*. 2009;91-B(5):565–576.
22. **Martin I**, **Miot S**, **Barbero A**, **Jakob M**, **Wendt D**. Osteochondral tissue engineering. *J Biomech*. 2007;40(4):750–765.
23. **Kanungo BP**, **Gibson LJ**. Density-property relationships in collagen-glycosaminoglycan scaffolds. *Acta Biomater*. 2010;6(2):344–353.
24. **Jeong CG**, **Zhang H**, **Hollister SJ**. Three-dimensional polycaprolactone scaffold-conjugated bone morphogenetic protein-2 promotes cartilage regeneration from primary chondrocytes in vitro and in vivo without accelerated endochondral ossification. *J Biomed Mater Res A*. 2012;100(8):2088–2096.
25. **Im G**, **Lee JH**. Repair of osteochondral defects with adipose stem cells and a dual growth factor-releasing scaffold in rabbits. *J Biomed Mater Res B Appl Biomater*. 2010;92(2):552–560.
26. **Onodera T**, **Momma D**, **Matsuoka M**, **et al**. Single-step ultra-purified alginate gel implantation in patients with knee chondral defects. *Bone Joint J*. 2023;105-B(8):880–887.
27. **Helwa-Shalom O**, **Saba F**, **Spitzer E**, **et al**. Regeneration of injured articular cartilage using the recombinant human amelogenin protein. *Bone Joint Res*. 2023;12(10):615–623.
28. **Zhou J**, **Xu C**, **Wu G**, **et al**. In vitro generation of osteochondral differentiation of human marrow mesenchymal stem cells in novel collagen-hydroxyapatite layered scaffolds. *Acta Biomater*. 2011;7(11):3999–4006.
29. **Rajan N**, **Habermehl J**, **Coté M-F**, **Doillon CJ**, **Mantovani D**. Preparation of ready-to-use, storable and reconstituted type I collagen from rat tail tendon for tissue engineering applications. *Nat Protoc*. 2006;1(6):2753–2758.
30. **Chen Z**, **Song Y**, **Zhang J**, **et al**. Laminated electrospun nHA/PHB-composite scaffolds mimicking bone extracellular matrix for bone tissue engineering. *Mater Sci Eng C Mater Biol Appl*. 2017;72:341–351.
31. **Chen Z**, **Wei J**, **Zhu J**, **et al**. Chm-1 gene-modified bone marrow mesenchymal stem cells maintain the chondrogenic phenotype of tissue-engineered cartilage. *Stem Cell Res Ther*. 2016;7(1):70.
32. **Chen Z**, **Zhang Q**, **Li H**, **Wei Q**, **Zhao X**, **Chen F**. Elastin-like polypeptide modified silk fibroin porous scaffold promotes osteochondral repair. *Bioact Mater*. 2021;6(3):589–601.
33. **Dawson JI**, **Wahl DA**, **Lanham SA**, **Kanczler JM**, **Czernuszka JT**, **Oreffo ROC**. Development of specific collagen scaffolds to support the osteogenic and chondrogenic differentiation of human bone marrow stromal cells. *Biomaterials*. 2008;29(21):3105–3116.
34. **Stark Y**, **Suck K**, **Kasper C**, **Wieland M**, **van Griensven M**, **Scheper T**. Application of collagen matrices for cartilage tissue engineering. *Exp Toxicol Pathol*. 2006;57(4):305–311.
35. **Rocha LB**, **Goissis G**, **Rossi MA**. Biocompatibility of anionic collagen matrix as scaffold for bone healing. *Biomaterials*. 2002;23(2):449–456.
36. **Xie J**, **Baumann MJ**, **McCabe LR**. Osteoblasts respond to hydroxyapatite surfaces with immediate changes in gene expression. *J Biomed Mater Res A*. 2004;71(1):108–117.
37. **Gleeson JP**, **Plunkett NA**, **O'Brien FJ**. Addition of hydroxyapatite improves stiffness, interconnectivity and osteogenic potential of a highly porous collagen-based scaffold for bone tissue regeneration. *Eur Cell Mater*. 2010;20:218–230.
38. **Wahl DA**, **Czernuszka JT**. Collagen-hydroxyapatite composites for hard tissue repair. *Eur Cell Mater*. 2006;11:43–56.
39. **Lu H**, **Cai D**, **Wu G**, **Zeng C**. Construction of tissue engineering cartilage with collagen/hydroxyapatite composite scaffolds loaded chondrocytes in vitro. *Chinese Journal of Clinical Rehabilitation*. 2006;10(25):177–180.
40. **Ducheyne P**, **Qiu Q**. Bioactive ceramics: the effect of surface reactivity on bone formation and bone cell function. *Biomaterials*. 1999;20(23–24):2287–2303.
41. **Green D**, **Walsh D**, **Mann S**, **Oreffo ROC**. The potential of biomimesis in bone tissue engineering: lessons from the design and synthesis of invertebrate skeletons. *Bone*. 2002;30(6):810–815.
42. **Burg KJ**, **Porter S**, **Kellam JF**. Biomaterial developments for bone tissue engineering. *Biomaterials*. 2000;21(23):2347–2359.
43. **Wozney JM**, **Rosen V**. Bone morphogenetic protein and bone morphogenetic protein gene family in bone formation and repair. *Clin Orthop Relat Res*. 1998;346:26–37.
44. **Reddi AH**. Morphogenesis and tissue engineering of bone and cartilage: inductive signals, stem cells, and biomimetic biomaterials. *Tissue Eng*. 2000;6(4):351–359.
45. **Babilotte J**, **Martin B**, **Guduric V**, **et al**. Development and characterization of a PLGA-HA composite material to fabricate 3D-printed scaffolds for bone tissue engineering. *Mater Sci Eng C Mater Biol Appl*. 2021;118:111334.
46. **Liuyun J**, **Chengdong X**, **Dongliang C**, **Lixin J**, **xiubing P**. Effect of n-HA with different surface-modified on the properties of n-HA/PLGA composite. *Appl Surf Sci*. 2012;259:72–78.
47. **Yin Hsu F**, **Chueh S-C**, **Jiin Wang Y**. Microspheres of hydroxyapatite/reconstituted collagen as supports for osteoblast cell growth. *Biomaterials*. 1999;20(20):1931–1936.
48. **Rodrigues CVM**, **Serricella P**, **Linhares ABR**, **et al**. Characterization of a bovine collagen-hydroxyapatite composite scaffold for bone tissue engineering. *Biomaterials*. 2003;24(27):4987–4997.

Author information

Y. Guo, PhD, Researcher,
Northwest University Chang An Hospital, Faculty of Life Sciences and Medicine, Northwest University, Xi'an, China;
Chang An District Hospital, Xi'an, China;
Engineering Research Center of Oral and Maxillary System Disease, School of Stomatology, Xi'an Medical University, Xi'an, China.

X. Peng, BSc, Researcher
Q. Liu, MS, Researcher
F. Chen, PhD, Professor
Z. Chen, PhD, Researcher
Northwest University Chang An Hospital, Faculty of Life Sciences and Medicine, Northwest University, Xi'an, China.

B. Cao, MS, Researcher, Jiangsu DiYun Medical Technology Co., Ltd, Suzhou, China.

S. Li, MD, Orthopaedic Surgeon
D. Zhi, MD, Researcher
S. Zhang, MD, Orthopaedic Surgeon
Northwest University Chang An Hospital, Faculty of Life Sciences and Medicine, Northwest University, Xi'an, China; Chang An District Hospital, Xi'an, China.

Author contributions

Y. Guo: Data curation, Methodology, Writing – original draft, Conceptualization, Formal analysis.
X. Peng: Data curation, Methodology.
B. Cao: Data curation, Methodology.
Q. Liu: Investigation, Methodology.
S. Li: Methodology, Resources.
F. Chen: Project administration, Supervision.
D. Zhi: Software, Supervision.
S. Zhang: Project administration, Supervision, Writing – review & editing.
Z. Chen: Project administration, Supervision.

D. Zhi, S. Zhang, and Z. Chen contributed equally to this work.

Funding statement

The authors disclose receipt of the following financial or material support for the research, authorship, and/or publication of this article: this work was supported by the National Natural Science Foundation of P. R. China (No. 32171329; reported by Z. Chen), Special Support Plan for High-level Talents (No. 334042000022; reported by F. Chen), Innovation Team Program in Shaanxi Province (No. 2019TD-032; reported by F. Chen), and Major special project of Qin Chuang Yuan (23LLRHZDZX0010; reported by Z. Chen).

ICMJE COI statement

F. Chen reports funding from the Special Support Plan for High-level Talents (No. 334042000022) and Innovation Team Program in Shaanxi Province (No. 2019TD-032), related to this study. Z. Chen reports funding from the National Natural Science Foundation of P. R. China (No. 32171329) and Major special project of Qin Chuang Yuan (23LLRHZDZX0010), related to this study.

Data sharing

The data that support the findings for this study are available to other researchers from the corresponding author upon reasonable request.

Ethical review statement

The New Zealand white rabbits (three months old, male:female = 1:1) were purchased from the Experimental Animal Center of Medical College of Xi'an Jiaotong University, and all procedures were approved by the Northwest University Institutional Animal Care and Use Committee (IACUC) (ACUC2013015).

Open access funding

The authors report that the open access funding for their manuscript was self-funded.

© 2025 Guo et al. This is an open-access article distributed under the terms of the Creative Commons Attribution Non-Commercial No Derivatives (CC BY-NC-ND 4.0) licence, which permits the copying and redistribution of the work only, and provided the original author and source are credited. See https://creativecommons.org/licenses/by-nc-nd/4.0/